GEOPHYSICAL RESEARCH LETTERS, VOL. 22, NO. 17, PAGES 2365-2368, SEPTEMBER 1, 1995

Observing tropospheric water vapor by radio occultation using the global positioning system

E.R.Kursinski[1,2], G.A.Hajj[2], K.R.Hardy[3], L.J.Romans[2] and J.T.Schofield[2]

Abstract. Given the importance of water vapor to weather, climate and hydrology, global humidity observations from satellites are critical. At low latitudes, radio occultation observations of Earth's atmosphere using the Global Positioning System (GPS) satellites allow water vapor profiles to be retrieved with accuracies of 10 to 20% below 6 to 7 km altitude and ~5% or better within the boundary layer. GPS observations provide a unique combination of accuracy, vertical resolution ($\leq$ 1 km) and insensitivity to cloud and aerosol particles that is well suited to observations of the lower troposphere. These characteristics combined with the inherent stability of radio occultation observations make it an excellent candidate for the measurement of long term trends.

Introduction

The need for high vertical resolution satellite observations of water vapor, providing global-scale coverage particularly over oceanic regions, has been discussed by Starr and Melfi (1991). Water vapor distribution often varies sharply in the vertical dimension as evidenced in the many forms of stratiform cloud systems 10^2-10^3 m thick, and the sudden change in water vapor concentration between the boundary layer and overlying free troposphere. The lack of adequate data limits our ability to analyze or simulate important aspects of the global climate system. Various investigators have identified GPS radio occultation measurements as a possible source of atmospheric water vapor data (Kursinski et al., 1991, 1993; Gorbunov and Sokolovskiy, 1993; Yuan et al, 1993). These occultation observations off high accuracy and a viewing geometry complementary to that of nadir vewing weather satellites. The work presented here provides the first global estimate of accuracy of tropospheric water vapor derivations from GPS occultations, calculated as a function of height, latitude and season. To obtain these estimates, it is assumed that independent pressure and temperature data from observations and meteorological analyses can be used to isolate the contribution of water vapor to the atmospheric refractivity profiles retrieved from occultation data. GPS occultation measurements are most sensitive to water vapor in the warmer regions of the troposphere, particularly in tropical regions where abundances are greatest, and their accuracy is limited primarily by uncertainties in the independent pressure and temperature data and errors in retrieved refractivity.

Resolution and Coverage

The Global Positioning System (GPS) was implemented to provide precise position determination. Yunck et al. (1988) pointed out that the GPS satellite constellation could be used to make radio occultation observations of Earth's atmosphere using one or more GPS receivers operating in low Earth orbit. With the present constellation of 24 GPS satellites, a single orbiting GPS receiver can observe of order 500 occultations per day spread across the globe. These observations have good vertical resolution at long wavelengths (~20 cm), providing a unique opportunity to routinely probe the troposphere using limb sounding geometry. Horizontal and vertical resolution perpendicular to the line of sight are roughly 1.5 km in the stratosphere, with vertical resolution improving to < 0.5 km near the surface. Along the line of sight, horizontal resolution is of order 200 km (Kursinski et al. 1993a).

Derivation of Water Vapor from Refractivity

In radio occultation, atmospheric refractive index profiles are retrieved from bending angle profiles derived from measured Doppler shift (Fjeldbo et al. 1971). As the index of refraction, n, is close to unity, it is convenient to define the refractivity, $N = (n-1) \times 10^6$. At microwave wavelengths, refractivity in Earth's lower atmosphere is related to atmospheric properties by the expression:

$$N = a_1 \frac{P}{T} + a_2 \frac{P_w}{T^2} \qquad (1)$$

where P is pressure in mbar, T is temperature in Kelvin, P_W is water vapor partial pressure in mbar, a_1 is 77.6 K/mbar and a_2 is 3.73×10^5 K^2/mbar. The uncertainty in the water vapor refractivity contribution to Eq. (1) is less than 0.5% (Thayer, 1974). At typical atmospheric temperatures and microwave wavelengths, the refractivity of pure water vapor is approximately 17 times greater than that of dry air so that, near the surface in the tropics, water vapor can contribute more than one-third of the total refractivity. Attenuation by particle scattering is negligible because GPS signal wavelengths are large (Kursinski et al., 1993b). The contribution of condensed water to atmospheric refractivity is small because its refractivity is only 25% (liquid) or 10% (ice) of that of an equivalent density of water vapor. Furthermore, condensed water abundances are a small percentage of vapor abundances. For example, very large liquid water abundances of 0.5 g/m^3, found at the top of stratiform cloud deck at the top of marine boundary layers, contribute approximately 1.4% to total water refractivity (Paluch et al. 1992).

Water Vapor Accuracy in the Lower Troposphere

It is clear from equation 1 that there is ambiguity between the contributions of P, T, and P_w to refractivity. However, water vapor profiles can be derived from refractivity profiles given independent estimates of P and T. Equation (1) can be rearranged to express P_W in terms of P, T, and N, to give:

$$P_w = \left(NT - a_1 P\right) \frac{T}{a_2} \qquad (2)$$

The sensitivity of water vapor partial pressure to errors in pressure, temperature and retrieved refractivity can be assessed by differentiating and manipulating Eq. (2) to give:

$$\frac{dP_w}{P_w} = \left(B+1\right)\frac{dN}{N} + \left(B+2\right)\frac{dT}{T} - B\frac{dP}{P} \qquad (3)$$

[1] Division of Geological and Planetary Sciences, California Institute of Technology,
[2] Jet Propulsion Laboratory, California Institute of Technology
[3] Lockheed Martin Missiles and Space, Palo Alto CA

Paper number 95GL02127
0094-8534/95/95GL-02127$03.00

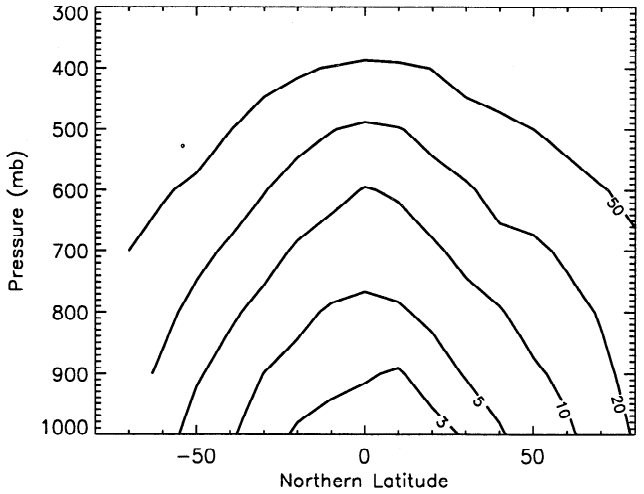

Figure 1. Dependence of the scaling factor, B (Eq. 3), on altitude and latitude for an annual mean temperature and water vapor climatology from Peixoto and Oort (1992).

where $B = a_1TP/a_2P_w$. Clearly B, and from Eq. (3), the accuracy of water vapor profiles derived from measurements of microwave refractivity, depends strongly on water vapor mixing ratio. The variation of B with altitude and latitude is shown in Figure 1.

Water vapor measurement errors can be derived from equation 3 given accuracy knowledge for N, P and T. Pressure and temperature error contributions to Eq (3) are correlated because they are related hydrostatically. Fractional pressure errors at a given altitude consist of a fractional pressure error at some boundary plus an error due to the integrated vertical structure of fractional temperature error. For a surface boundary, the total fractional pressure error at height, z, can be written as

$$\frac{\delta P}{P} = \frac{\delta P_s}{P_s} + \int_0^z \frac{\delta T\, dz}{T\, H} \qquad (4)$$

where H is the pressure scale height and $\delta P/P$, $\delta P_s/P_s$ and $\delta T/T$ are fractional errors in pressure, surface pressure and temperature. The maximum net error in Eq (3) occurs when $\delta T/T$ varies randomly with height and the second term on the RHS of Eq. (4) contributes little relative to the temperature term in Eq. (3). In this analysis, we therefore ignore the temperature error term in Eq. (4) and assume an rms surface pressure error of 3 mbar.

The determination of the accuracy with which tropospheric temperature can be measured and modeled has received much attention. Passive remote sounding measurements give rms errors typically ranging from 1 to 3 K relative to radiosonde measurements, depending on the instrument, the retrieval scheme, altitude, cloudiness and vertical temperature structure (Phillips et al. 1988; Kelly et al., 1991). The rms difference between lower troposphere temperatures in weather model analyses (specifically 6 hour forecasts) and radiosonde measurements ranges from 1 to 2 K (Andersson et al., 1991; Kelly et al., 1991). As radiosonde data are a primary input to the models, model accuracies in regions devoid of radiosondes will presumably be worse. In addition, radiosonde observations themselves are imperfect so estimates of accuracy made through comparison with radiosondes must be optimistic. The rms temperature error is assumed to be 1.5 K in this analysis.

To complete the water vapor error estimate, a retrieved refractivity error estimate is required. Random and systematic errors in refractivity are introduced by receiver thermal noise, clock instabilities, ionospheric correction residual errors, and the neglect of horizontal structure in the Abel transform retrieval. Based on several studies, the dominant source of error in the troposphere is expected to be the neglect of horizontal structure (Kursinski et al. 1993a,b; Gorbunov and Sokolovskiy, 1993; Vorob'ev and Krasil'nikova, 1993; Hardy et al. 1994). To characterize refractivity errors, we have simulated retrievals using both temperature and water fields obtained from a 40 km resolution NMC regional forecast ETA model (Janjic, 1990; Mesinger et al. 1988), modified by M. Zupanski for AIRS (Atmospheric Infrared Sounder) data simulation activities. Simulated measurements were generated by raytracing signal paths from GPS satellites to a receiver in low Earth orbit through the model atmospheric structure. Profiles of refractivity were then retrieved from the measurements using the Abel transform assuming spherical symmetry (Fjeldbo et al., 1971). The retrieved refractivity error statistics of figure 2 show that errors are of order 0.2% above 500 mbar and increase rapidly at lower levels due to increasing horizontal humidity gradients. At the top of the tradewind inversion (~800 mbar) a layer roughly 200 to 300 meters thick can contain vertical refractivity gradients that are large enough for critical refraction to occur. Signal paths whose tangent heights lie within such a layer cannot emerge from the atmosphere. The current implementation of the retrieval scheme is unable to derive refractivity accurately below critically refracting layers, so that only profiles without critical refraction are included in figure 2 below 800 mbar. Theoretically, only the portion of the refractivity profile within the critically refracting layer should be inaccessible to improved Abel transform retrievals.

If we assume that the refractivity, temperature and pressure error contributions to the water vapor retrieval error discussed above are independent, Eq. (3) becomes:

$$\frac{\sigma_{P_w}}{P_w} = \left[(B+1)^2 \left(\frac{\sigma_N}{N}\right)^2 + (B+2)^2 \left(\frac{\sigma_T}{T}\right)^2 + B^2 \left(\frac{\sigma_{P_s}}{P_s}\right)^2 \right]^{\frac{1}{2}} \qquad (5)$$

where σ_a is the standard deviation of quantity, a. Contours of water vapor profile error, derived from equation (5) for annual mean water vapor and temperature climatologies, are shown in Figure 3.

Low Latitude Water Vapor Retrievals

In order to examine the potential of GPS occultations for low latitude water vapor retrievals given realistic temperature

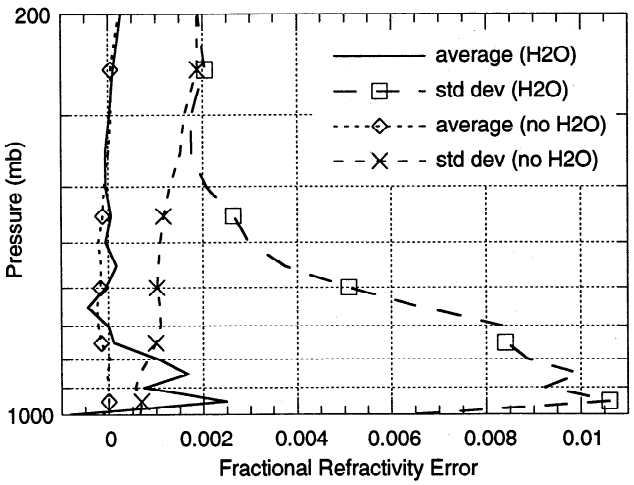

Figure 2. Fractional refractivity error estimated using a high resolution regional atmospheric model to generate approximately 100 simulated measurements and characterize the effects of horizontal refractivity structure on the Abelian retrieval process (see text). Profiles of mean retrieval error and error standard deviation are given for the entire set of simulations, both with and without the contribution of water vapor to refractivity.

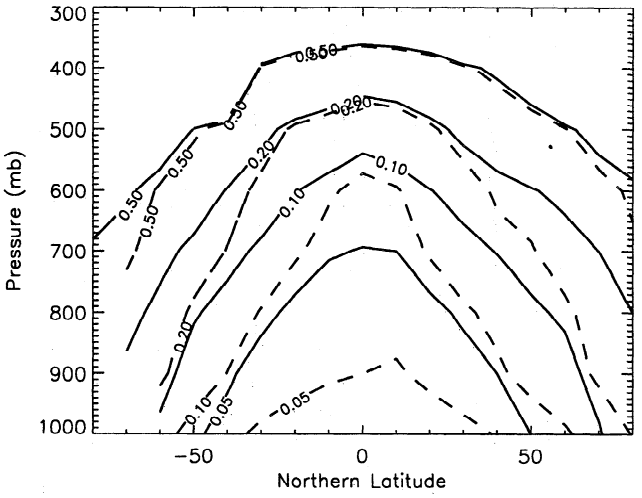

Figure 3. Estimated meridional dependence of fractional water vapor accuracy. Solid contours show errors due to 1.5 K temperature and 3 mbar surface errors. Dashed contours include the additional refractivity errors shown in Figure 2. Water vapor and temperature climatologies are annual means from Peixoto and Oort (1992).

and pressure variations, we have used 63 radiosonde soundings from Hilo, Hawaii, spanning the month of July 1991, to construct a short, single location, tropical climatology. To simulate errors in the derivation of humidity from retrieved refractivity due to temperature and pressure fluctuations, given a good mean pressure/temperature profile climatology, profiles of water vapor were derived from refractivity profiles calculated for each radiosonde sounding using the mean of all 63 soundings for the temperature and pressure estimates required by Eq. (2). The mean relative humidity profile for the month and the standard deviation from the mean, measured by the radiosondes, are shown in Figure 4a. The measured vertical structures of the standard deviation of pressure and temperature over the month are shown in Figure 4b. Overall the temperature fluctuations are similar to the 1.5 K rms error assumed above while the surface pressure variation is much smaller than the 3 mbar used above. The rms fractional error in water vapor derived in this simulation is shown in Figure 4c, both with and without the retrieved refractivity error of figure 2. The results of Figure 4c are generally consistent with the low latitude estimates of figure 2, with sensitivities of 20% or better achieved up to altitudes of 6 to 7 km. Sharp error increases near 2 and 4 km altitude are caused by day-to-day variations in the altitude of the inversion at the top of the boundary layer. Sensitivities below the tradewind inversion suggest that water vapor abundances within the convective boundary layer could be derived to the 1 to 5% level provided accurate retrieved refractivities are available in this region. This simulation of water vapor accuracy is successful because of the low variability of tropical atmospheric structure, but is conservative in that model atmospheric analyses at low latitudes should represent pressure and temperature structure more accurately than simple climatological averages.

Climatological Applications

Despite the fundamental role played by water in weather and climate, an adequate climatology of atmospheric water vapor does not exist. Radiosondes presently provide most of the high vertical resolution profiles of humidity with a highly inhomogeneous, land-biased spatial distribution. In the lower troposphere, GPS observations deliver hundred meter to one km vertical resolution with global coverage and 100-200 km horizontal averaging. This vertical resolution lies between that of radiosondes and current satellite remote sounding instruments and should yield a significant improvement in the vertical scales observable globally. In addition, horizontal averaging produces profiles that are more representative climatologically than point measurements. Finally, insensitivity to particulates allows GPS occultations to measure humidity structure representative of the entire range of climatological variation by retrieving water vapor profiles below clouds.

The GPS water vapor retrieval accuracies of Figures 3 and 4 at low latitudes compare favorably with goals of 5 and 10% established by Starr and Melfi for the boundary layer and overlying troposphere respectively, and are generally conservative, provided the problem of retrieval through critical layers is solved. Changes in water vapor abundance at low latitudes in the lower and mid-troposphere have been identified as reliable indicators of modeled climate change (Santer et al., 1990; Schlesinger et al., 1990). These are precisely the regions of greatest accuracy for GPS occultations.

Averaging GPS-derived humidities regionally and temporally to examine climatological behavior will reduce random errors and improve upon the accuracies summarized in Figures 3 and 4c, although improvements will ultimately be limited by systematic errors in the temperature, pressure and refractivity data used in deriving water vapor via Eq. (2). For the refractivity retrieval simulation presented in Figure 2, the profile of mean error is much smaller than the standard deviation of individual profile errors at all levels, suggesting that regionally averaged refractivity structure may be more accurate than individual refractivity profiles. Biases in estimates of temperature are difficult to quantify. Biases between NMC and ECMWF model analyses are of order 0.5 K or less in the lower troposphere (Kasahara and Mizzi, 1992). A comparison between radiosonde temperatures and those derived from the HIRS (infrared) and MSU (microwave) instruments on the NOAA-9 & 10 satellites indicate that biases at mid and low latitudes in the lower troposphere are generally 1 K or less (Flobert et al., 1991). A factor of 3 improvement in accuracy gained from av-

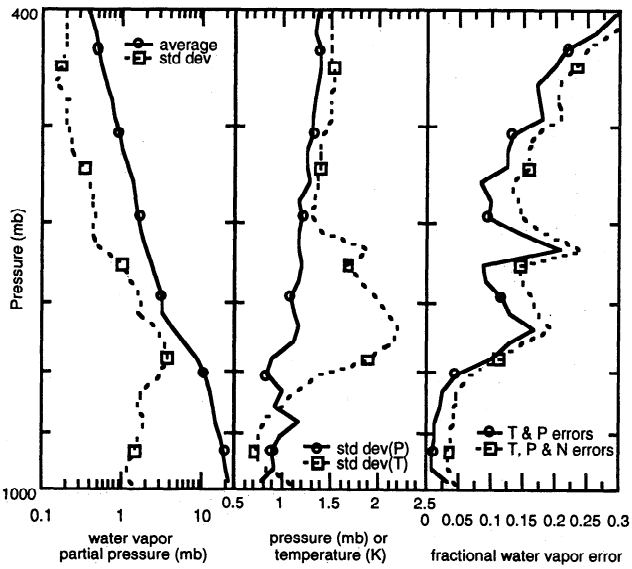

Figure 4. Estimated retrieval accuracy based on 63 radiosonde profiles from Hilo, Hawaii for July 1991. a: Average and standard deviation of radiosonde water vapor partial pressure data, b: Standard deviation of radiosonde temperature and pressure variations. c: Simulated accuracy of retrieved water vapor partial pressure. The solid curve shows errors due to temperature and pressure errors alone, whereas the dotted line also includes the refractivity error of Figure 2.

eraging, equivalent to a temperature bias of 0.5 K, would give specific humidity accuracies of better than 1.5% within the low latitude boundary layer and raise the 10% accuracy criterion for climatological utility by 3 km.

Conclusions

We have presented a first order overview of the resolution and accuracy with which water vapor structure can be derived from GPS occultation observations. These observations are extremely sensitive to water vapor, but their accuracy is limited by errors in pressure, temperature and retrieved refractivity. Accuracies are a strong function of water vapor abundance and the best measurements will be obtained in the warmer regions of the troposphere. GPS observations will yield little information on humidity in the upper troposphere. Instead, they will be used to determine density, pressure and temperature structure. The best humidity data will be obtained at low latitudes in the middle and lower troposphere where individual profile accuracies of better than 5% in the boundary layer and 20% up to 6 or 7 km altitude may be achieved. Mid-latitude accuracies will depend upon season. At 45° latitude, the altitude of 20% accuracy varies from approximately 5 km in the summer to 2-3 km in the winter hemisphere. For climatological investigations, averaging has the potential to improve upon these individual profile accuracies. Given its unique combination of good vertical resolution and insensitivity to clouds, this class of observations will improve our knowledge of the vertical humidity structure of the warmer troposphere significantly, particularly over regions such as the oceans where radiosonde coverage is sparse or nonexistent.

Acknowledgements. The research described in this publication was largely performed at the Jet Propulsion Laboratory, California Institute of Technology, supported jointly by the National Aeronautics and Space Administration and Caltech through the Caltech President's fund. Dr. Hardy was supported under the Lockheed Martin independent research program.

References

Andersson E., A. Hollingsworth, G. Kelly, P.Lönnberg, J. Pailleux and Z. Zhang, Global Observing system experiments on operational statistical retrievals of satellite sounding data, *Mon. Weath. Rev.*, ***119***, 1851-1864, 1991

Fjeldbo G., A.J. Kliore, and V.R. Eshleman, The neutral atmosphere of Venus as studied with the Mariner V radio occultation experiments, *Astronom J., 76*, 123-140, 1971

Flobert, J.F., E.Andersson, A.Chedin, A.Hollingsworth, G.Kelly, J.Pailleux and N.A.Scott, Global data assimilation and forecast experiments using the improved inversion method for satellite soundings, *Mon. Weath. Rev.*, ***119***, 1881-1914, 1991

Gorbunov, M.E. and S.V. Sokolovskiy, Remote sensing of refractivity from space for global observations of atmospheric parameters, *Report 119, Max-Planck-Institut fur Meteorologie.*, 1993

Hardy, K.R., G.A.Hajj and E.R.Kursinski, Accuracies of atmospheric profiles obtained from GPS occultations, *Intern. J. Sat. Comm., 12*, 463-473, 1994

Janjic, Z.I., The step-mountain coordinate physical package, *Mon. Weath. Rev., 118*, 1429-1443, 1990

Kelly G., E. Andersson, A. Hollingsworth, P.Lönnberg, J. Pailleux and Z. Zhang, Quality control of operational physical retrievals of satellite sounding data, *Mon. Weath. Rev., 119*, 1866-1880, 1991

Kasahara, A. and A.P.Mizzi, Estimates of tropical analysis differences in daily values produced by two operational centers, *Mon. Weath. Rev., 120*, 279-302, 1992

Kursinski, E.R., G.A.Hajj and K.R.Hardy, Moisture profile information from radio occultation measurements, *Eos Trans. AGU , 72*, 372, 1991

Kursinski E.R., G.A. Hajj, and K.R. Hardy, Temperature or moisture profiles from radio occultation measurements, *Proc. of the 8th Symp. on Meteorological Observations and Instrumentation*, Am. Met. Soc., pp. J153-J158, Anaheim, CA, Jan. 17-22, 1993a

Kursinski E.R., G.A. Hajj, and K.R. Hardy, Atmospheric profiles from radio occultation measurements of GPS Satellites, *Proc. of the SPIE Symp. on Optical Engineering and Photonics in Aerospace Science and Sensing*, paper no. 1935-13, SPIE, Orlando, FL, 1993b.

Mesinger, F., Z.I.Janjic, S.Nickovic, D. Gavrilov, D.G.Deaven, The step-mountain coordinate-model description and performance for cases of alpine lee cyclogensis and for a case of an appalachian redevelopment, *Mon. Weath. Rev., 116*, 1493-1518, 1988

Paluch, I.R., D.H. Lenschow, J.G.Hudson and R.Pearson, Transport and mixing processes in the lower troposphere over the ocean, *JGR, 97*, 7527-7541, 1992

Peixoto, J.P. and A.H.Oort, *Physics of Climate*, 520 pp., Am. Inst. Phys, New York, 1992

Phillips, N., J. Susskind and L. McMillin, Results of a joint NOAA/NASA sounder simulation study, *J. Atm.Oceanic Tech., 5*, 44-56, 1988

Raval, A. and V. Ramanathan, Observational determination of the greenhouse effect, *Nature, 342*, 758-761, 1989

Santer, B.D., T.M.I Wigley, M.E.Schlesinger and P.D. Jones, Multivariate methods for the detection of greenhouse-gas-induced climate change, in *Greenhouse-Gas-Induced Climatic Change: A Critical Appraisal of Simulatiuons and Observations*, edited by M.E.Schlesinger, Elsevier Science Publishers, Amsterdam, 1990

Schlesinger, M.E., T.P.Barnett and X.J.Jiang, On greenhouse gas signal detection strategies, in *Greenhouse-Gas-Induced Climatic Change: A Critical Appraisal of Simulations and Observations*, edited by M.E.Schlesinger, Elsevier Science Publishers, Amsterdam, 1990

Starr D.O'C. and S.H.Melfi, A strategic research plan for the GEWEX Water Vapor Project (GVaP), NASA Conference Publication 3120, May, 1991

Thayer, G.D., An improved equation for the radio refractive index of air, *Radio Sci., 9*, 803-807, 1974

Vorob'ev V.V. and T.G. Krasil'nikova, An estimation of accuracy of recovery of atmospheric refrctivity from measurements of doppler shifts at frequencies used in the Navstar system, *Ivestia AN. Fizica Atmosfery i Okeana, 29*, 626-633, 1993

Yuan, L.L., R.A.Anthes, R.H.Ware, C.Rocken, W.D.Bonner, M.G.Bevis and S. Businger, Sensing climate change using the global positioning system, *JGR, 98*, 14,925-14,937, 1993

Yunck, T.P., G.F.Lindal and C.H.Liu, The role of GPS in precise earth observation, *Proc of IEEE Position, Location and Navigation Symposium*, Orlando FL, 1988

E.R.Kursinski, G.A.Hajj, L.J.Romans and J.T.Schofield, Jet Propulsion Laboratory, California Institute of Technology, Pasadena CA 91109 (e-mail: erk@mercu1.caltech.edu; hajj@cobra.jpl.nasa.gov; ljr@cobra.jpl.nasa.gov; tim@scn1.jpl.nasa.gov)

K.R.Hardy, Lockheed Martin Missiles and Space, Palo Alto CA 94304-1187 (email: ken_hardy@mm.rdd.lmsc.lockheed.com)

(Received February 9, 1995; revised April 20, 1995;
accepted June 15, 1995)